https://doi.org/10.2352/ISSN.2169-4451.2019.35.42

The Optical Properties of the Woodburytype – An Alternative Printing Technique Based on a Gelatine/Pigment Matrix

D. J. Leech, W. Guy, S. Klein, Centre for Fine Print Research, University of the West of England, Bristol, BS3 2JT, United Kingdom

Abstract

The Woodburytype is a 19th century photomechanical technique, producing high-quality continuous-tone prints that use a mixture of pigment and gelatine as a relief print, in which the variation in height of the print produces the tone and contrast. We propose a phenomenological optical model for the process based on Kubelka-Munk theory that considers the ink formulation, the print height and the substrate surface in order to provide the ideal combination of printing depth and contrast.

Introduction

Printing methods have traditionally been utilised to mass produce items - at a low cost and with a large throughput. Both modern and more traditional processes, including screen, gravure and inkjet printing, have all been exploited across a broad number of scientific fields, such as for the production of flexible electronics [1], biosensors [2] and optical lenses [3]. Therefore, knowledge of these processes and their alternatives can be useful in determining not only the optimal printing method to attain the highest yield and throughput, but also for the identification of other possible applications.

In 1864, Walter B. Woodbury patented a method to print continuous tone photographic images from an intaglio/relief printing plate [4]. He licensed his method to various companies. When H. Barden Pritchard visited ‘The Woodbury Permanent Printing Company at Kent Gardens’ in 1882, he reported that 30 000 prints could be made in a day, which made them the main supplier for portraits between ‘electioneering orders and orders connected with Royal marriages’ [5]. Pritchard describes the steps for Woodburytype in an industrial setting, i.e. at The Woodbury Permanent Printing Company, as follows:

- A light sensitive gelatine film is put under a negative in a printing frame and printed in the sun.
- The unhardened gelatine is washed off in warm water. After hardening with alum, the film is mounted on a glass plate to dry.
- The dry film is stripped off and transferred into a steel tray.
- The steel tray is put into a press and a lead plate is pushed into the tray with a pressure between 150 to 500 tons which transfers the gelatine relief into the lead plate. Step 4 is repeated until enough lead plates are produced to fill the Woodbury printing press.
- The Woodbury printing press is a table revolving on a pivot with a number of printing presses mounted at the margin. The printer opens each press, pours a certain amount of warm pigmented gelatine on the oiled lead plate, puts a piece of paper on top, closes the press and rotates the table to repeat the procedure until he has reached the first press again.
- By then the gelatine has set, the print is removed, transferred to another room where it is dried, hardened, trimmed and mounted.

Commercial Woodburytype printing had disappeared by about 1900 [6]. The labour intensive postprocessing of the print (hardening, trimming and mounting) made it too costly to compete with halftoning prints [7], where no post-processing was required and text and images could be printed at the same time. Woodburytype today is no longer printed from lead plates. The most common modern practice to manufacture a Woodbury printing plate is to CNC mill the plate. The print is pulled from this milled printing plate or a silicon cast of the milled plate which is filled with the pigmented gelatine ink. After the ink has dried, the tone of the print is achieved by variations of the print height and therefore of the probability that photons are absorbed or scattered as they pass through the print. The higher the attenuation coefficient and the longer the light path through the medium, the darker the tone. We suggest a simple optical model to predict the optimal carbon black pigment concentration and therefore ink composition for a given printing plate depth, in order to achieve the largest possible grayscale – which is currently the most involved and time-consuming process in the printing cycle.

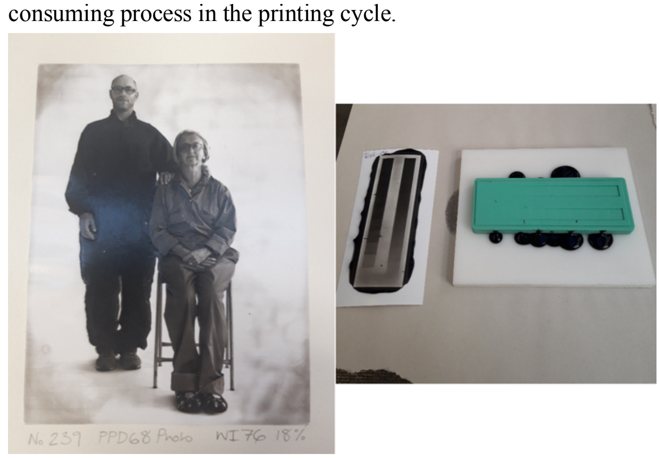

Figure 1. *Two examples of the Woodburytype printing process, using inks of pigment concentration of 0.015% (left) and 0.025% (right). The step-wedge printing plate gives a simple reflection of the Woodburytype process, whereby the deeper troughs are translated into darker tones. This approach can also be used to recreate more complex images, such as the figures on the left, in a similar manner.*

Ink Formulation

Historic ink formulations, as in Ref. [8], X-ray fluorescence analysis and attenuated total reflectance Fourier-transform infrared spectroscopy, as in Ref. [9], show that Woodburytype inks in prints historically contain gelatine and pigment – lacking the more typical imaging metals, such as in silver halide photographic prints. The gelatine inks used here consist of 17.5 wt% of gelatine, 82.5 wt% of de-ionised water and 0.005 to 0.1 wt% of carbon black. The gelatine used was Rousselot 250 bloom food grade gelatine (Rousselot, used as received) and the carbon black was XPB 430 (Orion engineered carbon, used as received), an easy-to-disperse carbon black pigment preparation with 50 wt% pigment content. Half of the deionised water was added to the gelatine and the mixture was left to swell. The pigment was dispersed in the rest of the water and added to the water gelatine mixture, when all the water was absorbed by the gelatine. The final mixture was melted in a low temperature oven at 50 °C. To age the gelatine, the ink was put into a fridge at 6 °C for 12 hours and then heated up to 40 °C for printing.

Print Process

In order to obtain quantitative data, we use a step-wedge silicon printing plate that consists of eleven equally spaced and adjacent steps with depths between 0 mm and 1 mm, as seen in Figure 1. These steps are 1 cm × 1 cm in width, to ensure they are larger than the viewing aperture of our optical measurement equipment. The printing process involves filling the plate with a surplus of the gelatine ink, placing paper onto the filled plate and transferring the ink to the paper by exposing it to pressure in a letter press until the ink has set. The compression time, between 5 to 10 minutes, depends on the amount of gelatine contained in the ink - a larger weight percentage will lead to a shorter setting time. As a release agent, lavender oil was applied to the plate prior to printing to ensure that the ink transfers to the paper surface. We use a glossy photographic microporous ink-jet paper (SKU PPD-68) in order to minimize ink absorption by the paper. Each print is repeated three times to ensure we obtain at least one print free from visually-obvious defects, such as bubbles of air that can be trapped in the ink during the printing process or tearing of the print edges, where the printing plate has not been cleanly pulled away.

CIELAB Measurements

To determine the grayscale, we used a Konica-Minolta FD-7 spectrometer to represent the data in the CIELAB coordinate system [10]. It is defined by three variables, L^*, a^* and b^*. L^* represents the 'lightness', ranging from 0 (dark) to 100 (light), a^* the green-red and b^* the yellow-blue colour components, that range from -100 to 100, respectively. These are mathematically accessed via the CIEXYZ colour space, comprised of the three tristimulus values X, Y and Z, that are similar but less perceptively uniform.

As we are currently concerned with monochromatic prints, we use only the value of L^*, which is linked to the Y tristimulus value via [11]

$$L^* = 116\, f\left(\frac{Y}{Y_n}\right) - 16, \tag{1}$$

where $Y_n = 85$, the Y value of the paper substrate we utilise, $\delta = 6/29$ and $f(t) = t^{\frac{1}{3}}$ if $t > \delta^3$ or $f(t) = \frac{t}{3\delta^3} + \frac{4}{29}$ if $t < \delta^3$. The tristimulus value Y itself has the form

$$Y = 100 \sum_\lambda \frac{R(\lambda) S(\lambda) \bar{y}(\lambda) \Delta\lambda}{S(\lambda) \bar{y}(\lambda) \Delta\lambda}, \tag{2}$$

where $S(\lambda)$ is the relative spectral power distribution, $R(\lambda)$ is the spectral reflectance factor and $\bar{y}(\lambda)$ is one of the three colour matching functions used in the CIEXYZ colour space. We utilise a standardised D65 illuminant, intended to represent average daylight with a correlated colour temperature of roughly T = 6500 K [10], and so $\bar{y}(\lambda)$ has a form given by the approximation in Ref. [12].

Kubelka-Munk Theory

Kubelka-Munk theory is a radiative transfer model that characterises the properties of optically turbid media such as paint or ink films. It models the layer as a homogeneous medium, rather than an ensemble of individual pigment particles, in order to ignore complex multiple-scattering effects and characterises the film with an absorption K and scattering coefficient S, per unit length [13]. It is assumed that these coefficients are uniform throughout the thickness of the film and that there are no prominent boundary effects, such that the plane has an effectively infinite width and length.

Multiple attempts have been made to link these Kubelka-Munk (KM) coefficients, K and S, with the properties of the individual pigment particles [11] [14] [15] [16] [17], however the exact relationship seems to vary greatly depending on the ratio between K and S. As such, Kubelka-Munk theory is seen as a purely phenomenological approach and is also therefore pigment dependent.

The reflectance $R(\lambda)$ of a film on a substrate can be predicted via the KM coefficients as [15]

$$R = \frac{1 - R_g(a - b\,\coth bSd)}{a - R_g + b\coth bSd}, \tag{3}$$

where

$$a = \frac{S+K}{S}, \quad b = \sqrt{a^2 - 1}. \tag{4}$$

These equations dictate how the reflectance changes with the substrate reflectance R_g (that ranges between 0 and 1 for a perfectly black and perfectly white diffuser, respectively) and film thickness, d. The reflectance of carbon black varies minimally in the visible region [18] and so we assume it is effectively constant across these wavelengths. The reflectance tends toward a set value R_∞, that describes a layer providing zero transmission, that can instead be calculated by

$$R_\infty = 1 + \frac{K}{S} - \sqrt{\left(\frac{K}{S}\right)^2 + 2\left(\frac{K}{S}\right)}. \tag{5}$$

It is through these reflectance values that we can link the CIELAB values to the KM coefficients and therefore parameterize the inks we are using.

The print height d of the Woodburytype print is of huge importance, as it varies to a greater degree than in a traditional print and an increasing film thickness ensures a greater chance of absorption and scattering events taking place. A known gelatine content in the ink formulation means that we can estimate the print height, purely from the trough depths of our printing plate. Using the fact that the steps have dimensions 1 mm × 1 mm × Z mm, where Z varies between 0.1 and 1 mm, the ratio between the volume of the gelatine and the total mixture should give us an estimate of the print height once dry. We neglect the presence of carbon as this represents, at most, 1% of the dry mixture. The ratio in this recipe is given by densities of ρ_{gel} = 1.3 g/cm^3 [19] so that the volume of gelatine in the recipe is V_{gel} = 15/1.3 = 11.5385 cm^3 and the ratio is V_{gel}/V_{tot} = 0.1415. Therefore, in the deepest step with height 1 mm, the print height should be $d = 0.1415 \times 1 = 0.1415$ mm = 142 μm. We assume that these heights are directly proportional to the step depth and scale based on this value. The gelatine print heights can also be measured by Scanning Electron Microscopy (SEM), as seen in Figure 2c, and show a similar trend to the above calculation.

Figure 3a shows the CIELAB results for thirteen differing inks. The pigment concentrations increase in rough steps of 0.005% carbon content below 0.02% and in steps of 0.02% above that, to closely map the sharp decay of the data at those lower pigment concentrations. The photographic paper used has a CIELAB brightness of $L^* = 93.3$ and provides an upper limit to the data set. As expected, the general trend is an exponential decay toward a minimum value of $L^* = 6.5$ with increasing pigment concentration, corresponding to the presence of a minimum reflectance value, R_∞.

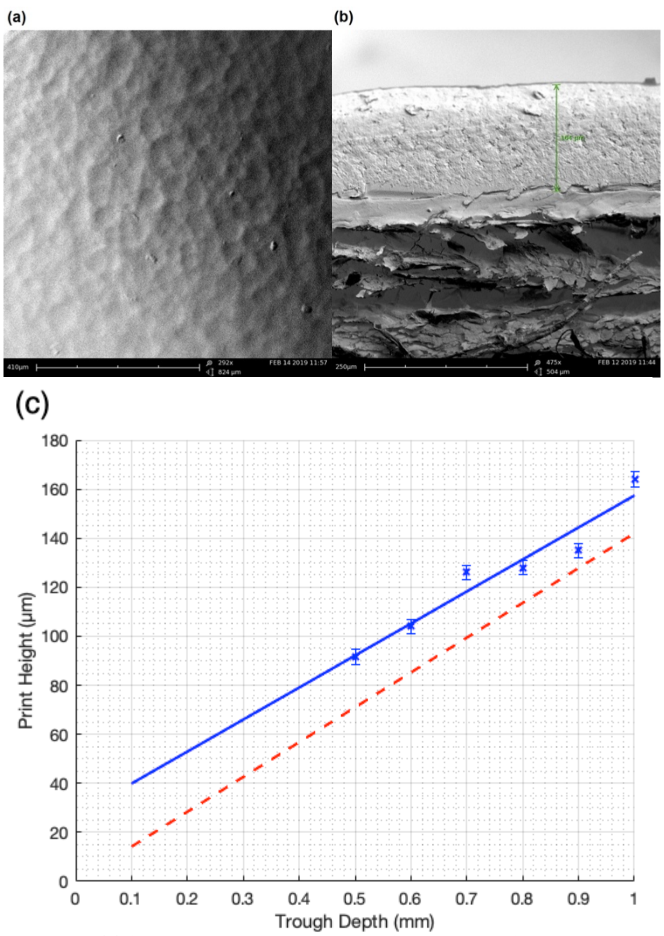

Figure 2. *(a) Scanning electron micrograph of the paper surface - as the surface is distinctly cratered, we can assume it will therefore provide a diffuse reflectance. (b) Example of the measurement of the gelatine print height, via imaging of the print 'edge-on'. Below the print is the paper, now split during the process of drying due to the constriction of the gelatine. (c) Dried print height against the depth of the trough on the printing plate. We take a general trend, the solid line, in order to minimise the variations in the print height. The dashed line represents the simple estimation based on the proportion of gelatine in the ink, as described in the text.*

Single Coefficient Fitting

Using the equations previously defined for reflectance, we can use various values of the KM coefficients, K and S, in order to predict the L^* curve for a particular concentration. If we assume that all particles dispersed in the gelatine matrix can be considered identical, we can define the absorption and scattering coefficients within the Kubelka-Munk theory in terms of the absorption and scattering cross sections

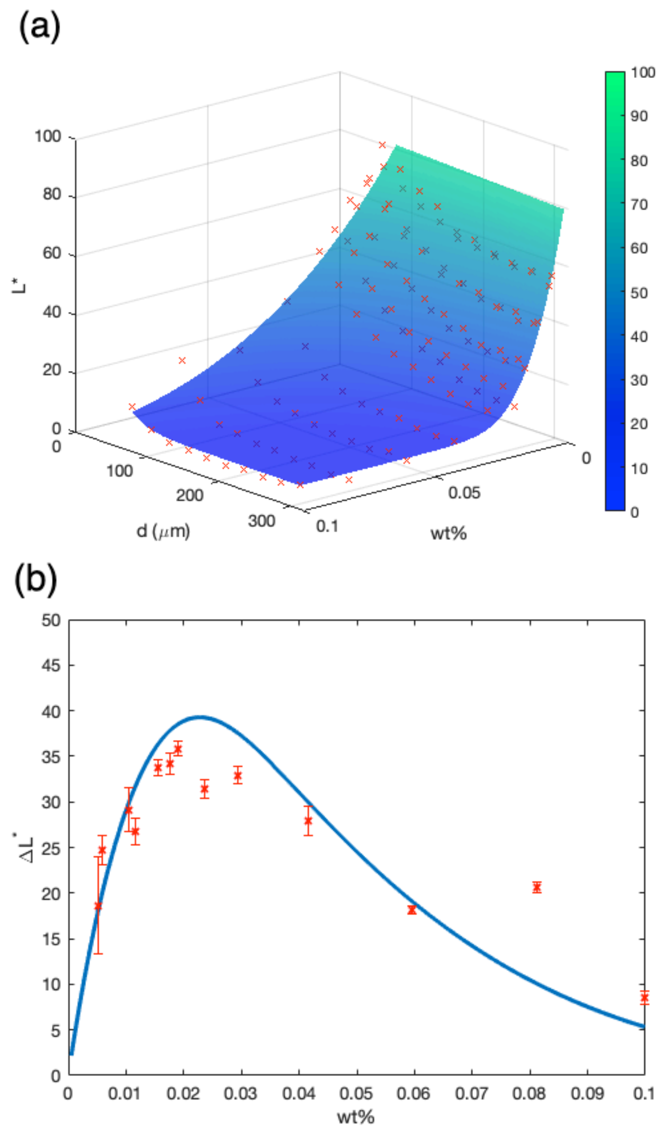

Figure 3. *(a) CIELAB results of the step-wedge prints for varying weight percentages, the data points are represented by the crosses. A higher concentration of pigment results in a darker print, as expected, and the prints in general tend toward a minimum non-zero L^* value. Note that additional fitting has been implemented, using the value of the paper reflection R_g. (b) The contrast of a step-wedge print, calculated as the max difference in L^*, for inks of varying weight percentage and comparing the data points against the curve predicted by the theory.*

$$K = f\frac{C_{Abs}}{V}, \qquad S = f\frac{C_{Sca}}{V}, \tag{6}$$

where V is the volume of one such particle and f is the particle volume fraction [18], that can be related to the particle weight fraction F via

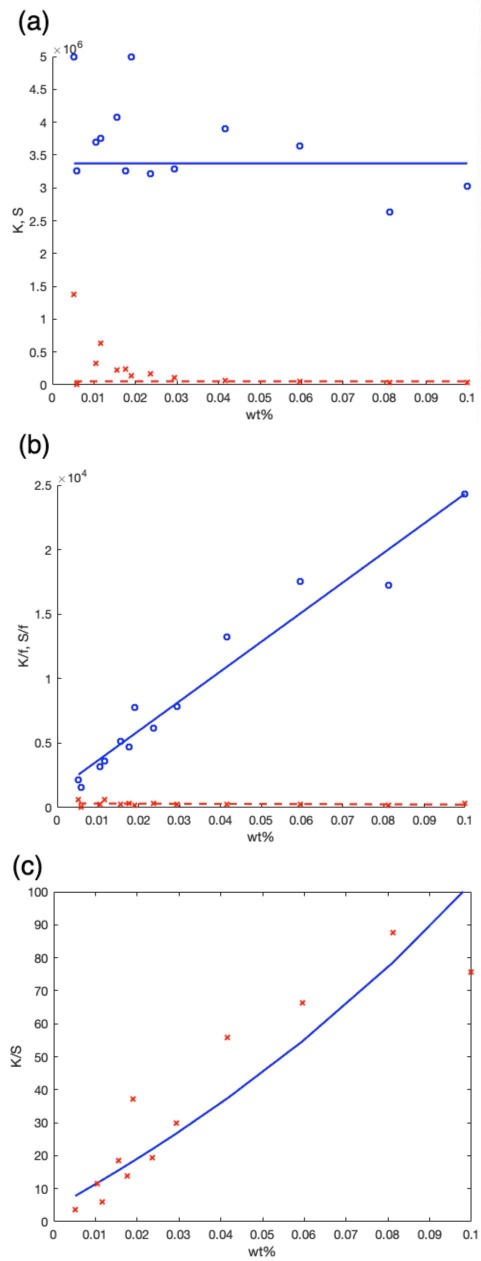

Figure 4. *(a) KM coefficients fitted per weight percentage and therefore per print. Blue circles represent the absorption term K and red crosses the scattering term S. The solid and dashed line represent the values of K and S, respectively, found previously in Figure 3a. (b) The variation in value in the KM coefficients per print, scaled by the volume fraction. A line of best fit, again solid for absorption and dashed for scattering, is added to highlight that the absorption term has a positive gradient and the scattering remains relatively constant and small, with a small negative gradient toward extremely weak pigment inks. (c) The Kubelka-Munk unit with varying weight percentage – showing both the data taken and the curve predicted by the fit in (b).*

$$f = \left[1 + \frac{\rho_{car}}{\rho_{gel}}\left(\frac{1-F}{F}\right)\right]^{-1}, \tag{7}$$

where ρ_{car} = 1.8 g/cm^3 [20] and ρ_{gel} = 1.3 g/cm^3 [19] and a particle weight fraction between 0.1% and 1.1%.

We then use these scaled KM coefficients to predict the L^* curve and use the mean squared error method to characterize the deviation from the data set. With *n* data points *y*, alongside the same number of calculated points *y'*, the mean squared error of such a data set is

$$MSE = \frac{1}{n}\sum_1^n (y - y')^2. \tag{8}$$

We minimise this value by varying the variable set $\{C_{Abs}/V,\ C_{Sca}/V,\ R_g\}$ to provide the best fit for the data set. We find this minimum exists for $C_{Abs}/V = 3.37 \times 10^6$, $C_{Sca}/V = 0.05 \times 10^6$ and $R_g = 0.52$ and is similar in magnitude to the results found in Ref. [18], with a slight underestimation of the absorption term. The results of this fitting can be seen in Figure 3a, against the original data set. The reflectance of the substrate is reduced to a single fitted number, rather than the proper reflectance of the paper, to allow for the model to be quickly applied to printing plates of varying depths, using the confirmed ink absorption and scattering terms as an anchoring point.

We can then extend this by plotting the full L^* dependence and discerning the grayscale range ΔL^* of each possible print, as the difference between the L^* values of the largest and smallest trough of our step-wedge, such that

$$\Delta L^* = L^*_{max} - L^*_{min}, \tag{9}$$

where L^*_{max} lies at the step with maximum depth (1 mm) and L^*_{min} lies at the step with minimum depth (0.1 mm). Figure 3b displays the results of such a dependence, comparing both the measured results and the theoretical expectation values, and shows the distinct region of inks that should provide the largest grayscale congregate around a weight percentage of 0.02%. The CIELAB results, averaged across three measurements, for three inks, including one with the largest ΔL value, can be seen in the Table below.

Multiple Coefficient Fittings

As a first approximation, we have ignored any of optical properties of the binding gelatine that comprises the majority of the print, justified by the hugely absorbent nature of the pigment used. However, it is feasible to assume that as the weight percentage decreases, the optical effects of the gelatine should emerge more prominently and the absorption and scattering coefficients could change.

We test this assumption by allowing the characteristic absorption and scattering, *K* and *S*, to vary with the weight percentage of the pigment. The value of the reflectance of the substrate R_g is assumed to be constant during this variation and takes

	STEP DEPTH (MM)									
WT%	0.1	0.2	0.3	0.4	0.5	0.6	0.7	0.8	0.9	1.0
0.0052	75.12	70.12	66.27	63.18	59.77	58.93	57.87	56.53	56.83	58.02
0.0190	53.12	41,78	33.89	29.29	25.2	23.11	19.05	17.27	16.25	16.45
0.0999	15.31	9.72	7.42	7.00	6.62	6.48	7.00	6.78	7.12	8.52

the value of the previous fitting. The results of this process can be seen in Figure 4a - each print and therefore ink formulation is now described by a unique set of KM coefficients. A comparison to the single coefficient fitting is represented by the solid lines. When the absorption and scattering coefficients are scaled by the volume fraction (Eq. (6)), as seen in Figure 4b, the linear relationship between the data points becomes more obvious. The absorption coefficient increases with increasing pigment concentration and the scattering coefficient has a mild negative gradient, increasing as the print optics become more dominated by the effects of the gelatine binder.

Overall, the values remain somewhat consistent above weight percentages of 0.02%, but scattering is enhanced below this value. This could be the result of the increase of the contribution of the optical properties of the background gelatine with decreasing pigment concentration. It results in a lower limit to our model that could explain the underestimation of the absorption given by the single coefficient fitting.

Conclusion

To reproduce the high quality of historical Woodburytypes, one important step is to determine the optimal pigment concentration of the ink, in order to generate prints with a good grayscale in the mid-tones. The pigment concentration is correlated to the relief height of the printing plate - the shallower the printing relief, the higher the pigment concentration needed. We used a Kubelka-Munk model for light propagation in the relief of a Woodburytype and found that two methods of fitting CIELAB L^* data against print height lead to similar values for absorption and scattering coefficients. This allows for a robust characterisation of the carbon black ink we utilise and provides a method of quickly deducing the pigment-load that produces the largest range of L^* values, knowing only the maximal depth of the printing plate. A pigment-load of 0.02wt% was found to give the maximum difference in the L* values for a step-wedge printing plate with a relief between 0.1 and 1 mm, however as the region of maxima in Figure 3b is somewhat flat, this allows for some tuning of the white point without losing the definition in the mid-tones. This simple phenomenological model will be used extensively to streamline the ink-making process for future printing plates with different relief depths and can be used as a basis for more complex Woodburytype approaches, such as full colour prints.

Bibliography

[1] D. Li, Y. Z. Zhang and W. Huang, "Printable Transparent Conductive Films for Flexible Electronics," *Advanced Materials,* vol. 30, no. 1704738, 2018.

[2] J. Li, F. Rossignol and J. MacDonald, "Inkjet printing for biosensor fabrication: combining chemistry and technology for advanced manufacturing," *Lab on a Chip,* vol. 15, pp. 2538 - 2558, 2015.

[3] J. Alamán, R. Alicante, J. I. Peña and C. Sánchez-Somolinos, "Inkjet Printing of Functional Materials for Optical and Photonic Applications," *Materials,* vol. 9, no. 910, 2016.

[4] W. B. Woodbury, "Producing Surfaces in Relief". London Patent 2338, 23rd September 1864.

[5] H. B. Pritchard, The Photographic Studios of Europe, London: Piper & Carter, 1882.

[6] B. Coe and M. Haworth-Booth, A Guide to Early Photographic Processes, London: Victoria & Albert Museum, 1983.

[7] F. E. Ives, "Photographic Block Methods," *Photographic News,* p. 13, 4th January 1884.

[8] Unknown, "The Woodbury Process: Sixth Article," *Photographic News,* 2nd May 1884.

[9] A. K. Dusan and C. Stulik, Woodburytype, Los Angeles: The Getty Conservation Institute, 2013.

[10] J. Schanda, Colorimetry: Understanding the CIE System, Vienna: CIE Central Bureau, 2006.

[11] L. E. McNeil and R. H. French, "Light scattering from red pigment particles: Multiple scattering in a strongly absorbing system," *Journal of Applied Physics,* vol. 89, no. 1, 2000.

[12] C. Wyman, P. P. Sloan and P. Shirley, "Simple Analytic Approximations to the CIE XYZ Color Matching Functions," *Journal of Computer Graphics Techniques,* vol. 2, no. 2, 2013.

[13] P. Kubelka and F. Munk, "Ein Beitrag zur Optik der Farbanstriche," *Zeitschrift für Technische Physik,* vol. 12, pp. 593 - 601, 1931.

[14] P. S. Mudgett and L. W. Richards, "Multiple Scattering Calculations for Technology," *Applied Optics,* vol. 10, pp. 1485 - 1502, 1971.

[15] M. Quinten, "The color of finely dispersed nanoparticles," *Applied Physics B,* vol. 73, pp. 317 - 326, 2001.

[16] L. Yang and B. Kruse, "Revised Kubelka-Munk theory. I. Theory and application," *Journal of the Optical Society of America A,* vol. 21, pp. 1933 - 1941, 2004.

[17] H. Granberg and P. Edström, "Quantification of the Intrinsic Error of the Kubelka-Munk Model Caused by Strong Light Absorption," *Journal of Pulp and Paper Science,* vol. 29, pp. 386 - 390, 2003.

[18] T. Tesfamichael, A. Hoel, G. A. Niklasson, E. Wäckelgård, M. K. Gunde and Z. C. Orel, "Optical characterization method for black pigments applied to solar-selective absorbing paints," *Applied Optics,* vol. 40, pp. 1672 - 1681, 2001.

[19] N. G. Parker and M. J. W. Povey, "Ultrasonic study of the gelation of gelatin: Phase diagram, hysteresis and kinetics," *Food Hydrocolloids,* vol. 26, pp. 99 - 107, 2012.

[20] "What is Carbon Black?," [Online]. Available: https://www.thecarycompany.com/media/pdf/specs/orion-what-is-carbon-black.pdf. [Accessed 4th March 2019].

Author Biography

Damien Jon Leech received his MSc and PhD in Physics from the University of Bath, in 2014 and 2018 respectively, researching 2D *materials and condensed matter theory. Since then he has worked within the Centre for Fine Print Research at the University of the West of England, focusing on the resurrection and modernization of late 19^{th}/early 20^{th} century printing and photographic techniques.*